IBRACON Structures and Materials Journal
Revista IBRACON de Estruturas e Materiais
ISSN 1983-4195 ismj.org

ORIGINAL ARTICLE

Numerical evaluation of dynamic load models of humans walking on building floors

Avaliação numérica de modelos de carga dinâmica de caminhada humana em pisos de edifícios

Rafael Nunes da Cunha[a]
Higor Sérgio Dantas de Argôlo[a]

[a] Universidade Federal de Sergipe – UFS, Instituto de Pesquisa sobre Desastres, Programa de Pós-graduação em Engenharia Civil, São Cristóvão, SE, Brasil

Received 26 July 2023
Revised 12 February 2024
Accepted 11 March 2024

Abstract: Composite steel and concrete floors are often susceptible to excessive vibrations caused by human activities because of their slender structural elements. To achieve a precise evaluation, it is necessary to incorporate the effects of dynamic loads in the computational model; however, it is difficult to predict this type of load. This study aims to analyze a set of human dynamic load models applied to four composite steel and concrete floors and verify which model can simulate the real load effects by comparing the numerical results obtained in this research with the experimental results obtained in other studies. It was possible to determine the dynamic model that yielded peak and root mean square accelerations closer to the experimental values for different analysis situations.

Keywords: composite steel and concrete floors, floor vibration, human walking, dynamic load models.

Resumo: Os pisos mistos de aço e concreto são frequentemente suscetíveis a vibrações excessivas devido a atividades humanas de caminhar por causa de seus elementos estruturais esbeltos. Para alcançar uma avaliação precisa, é necessário incorporar os efeitos das cargas dinâmicas no modelo computacional, porém, é difícil prever este tipo de carregamento. Assim, o presente trabalho tem como objetivo estudar os modelos dinâmicos de carga humana aplicadas em quatro pisos mistos de aço e concreto e verificar qual melhor representa estas ações ao comparar resultados numéricos de aceleração, obtidos nesta pesquisa, a referências experimentais, obtidos em outros trabalhos. Foi possível definir o modelo dinâmico que conduziu a resultados de acelerações de pico e RMS mais próximos dos experimentais para diferentes situações de análise.

Palavras-chave: pisos mistos de aço e concreto, vibração de pisos, caminhar humano, modelos de carregamento dinâmico.

How to cite: R. N. Cunha and H. S. D. Argôlo, "Numerical evaluation of dynamic load models of humans walking on building floors," *Rev. IBRACON Estrut. Mater.*, vol. 17, no. 5, e17512, 2024, https://doi.org/10.1590/S1983-41952024000500012.

1 INTRODUCTION

1.1 Background

Composite steel and concrete structures have been widely applied in civil engineering to satisfy new architectural trends including the use of slender structural elements and open-plan layouts with few internal partitions. These structure types also satisfy the need for fast building construction, particularly for commercial use [1], [2].

Recent developments in structural concepts using composite steel and concrete structures have resulted in significant reductions in stiffness and damping effects. Consequently, the fundamental frequency is reduced, resulting in structures that are more susceptible to problems related to excessive vibration [3]. This is because the most common excitation frequencies of human activities are close to the fundamental frequencies of these types of structures [4].

Corresponding author: Rafael Nunes da Cunha. E-mail: rafael.cunha@ctec.ufal.br
Financial support: None.
Conflict of interest: Nothing to declare.
Data Availability: The data supporting the findings of this study are available from the corresponding author, R. N. Cunha, upon reasonable request.

The proximity between the fundamental frequency of the structure and the excitation frequencies may accelerate floor vibrations, disturb users in the environment, and result in a loss of productivity. However, acceptable vibration levels vary among people owing to different levels of perception and the types of activities performed [5], [6].

Corrective methods always cause inconvenience to users of the structure. Although the main remedial measures include an increase in stiffness or structural damping [7], the use of passive control systems has increased in recent decades owing to their ease of application and reduced dimensions [8], [9]. However, the adoption of corrective methods always entails additional costs, which can render the structure infeasible from an economic perspective [10]. Checking for excessive vibration has become a determining factor in the design stage and an accurate description of human actions is crucial for advances in structural vibration studies. Therefore, the main aim of this study was to determine the most realistic human dynamic model for numerical vibration analysis of human comfort based on experimental results.

1.2 Floor vibration

In the 1980s, the number of floor vibration studies increased with the proposal of new and simplified analysis methods related to different human activities. These methods suggest the limits of acceptability defined by the peak acceleration (a_p) [7], [11], [12] and the root mean square acceleration (a_{rms}) [13]–[15]. However, simplified methods may not be suitable for all analyses; therefore, accurate methods, such as finite element methods, should be adopted with analytical functions that represent human activities.

Experimental tests have increased our understanding of the dynamic forces caused by human walking. Thus, it is possible to determine the dynamic parameters of walking activities based on the instrumentation of the structures. Based on these parameters, sinusoidal functions that vary over time can be applied to describe human walking activities [16], [17]. Tests have been conducted on treadmills [18], [19], outdoor pedestrian bridges [16], [20], composite steel and concrete platforms [21]–[23], and real structures [24]–[26], and many new human dynamic models have been proposed.

The floor properties are also important factors in dynamic analysis, such as the damping ratio [9] and modal mass [27]. Experimental tests were conducted on different composite steel and concrete floors to analyze the dynamic responses of these structures under human loads [28]–[34]. Different types of dynamic responses were observed based on the fundamental frequency of the floor. Floors with a fundamental frequency below 9 Hz were classified as having a low fundamental frequency. Floors with fundamental frequencies higher than 9 Hz were defined as having a high fundamental frequency. Despite these improvements, experimental studies may not be feasible owing to technical or cost constraints. Therefore, as a relatively simple and low-cost procedure, numerical studies are important for the analysis of dynamic loading models [35]–[37] and general numerical modeling [29]–[31].

Barrett [29] proposed an alternative to avoid modeling steel deck ribs. This methodology uses a parameter, PM, that modifies the concrete properties in the direction of the ribs. An equivalent cross-section of the steel deck slab must be defined that maintains the original height and total area of the steel deck for a unitary length, and the concrete must be modeled as an orthotropic material. The PM parameter is calculated as the ratio of the moment of inertia of the equivalent cross-section to that of the slab section. The PM parameter increases the longitudinal elasticity modulus of the concrete floor slab in the rib direction [30], [31].

Based on the studies described above, the aim of the present study was to evaluate the quality of the vibration acceleration results produced by different numerical models of human walking for different floor situations. Dynamic models were applied to four composite steel and concrete floors, and the numerical results were compared with experimental studies available in the literature.

2 METHODOLOGY

The aim of the present study was to identify a dynamic load model that leads to acceleration results that are closer to experimental results based on composite steel and concrete floor walking tests. Thus, a group of dynamic load models describing human walking behavior was selected from the literature that, along with a set of steel, composite steel, and concrete floors. These floors were numerically modeled according to the properties described in the respective papers. The dynamic load models were applied, and the numerical acceleration results were compared to the experimental results. The models are described in the following sections.

2.1 Mathematical models of human walking load

Mathematical functions with temporal variations were used to describe human walking activities. These functions are defined using dynamic coefficients (α), phase angles (φ), and human weight (Q). In addition, to better describe the

activities, it is necessary to know the step frequency of the activity (f_s) and the step length. Bachmann and Ammann [4] described these parameters with multiple values according to walking speed, as shown in Table 1.

Table 1. Human walking parameters [4].

	f_s (Hz)	Speed (m/s)	Step length (m)
Slow walk	1.7	1.1	0.6
Normal walk	2.0	1.5	0.75
Fast walk	2.3	2.2	1.0

Dynamic loads were applied in two different ways: considering only temporal variation, with a single load in the central position of the walking path (Figure 1a), and considering temporal and spatial variations along the walking path (Figure 1b).

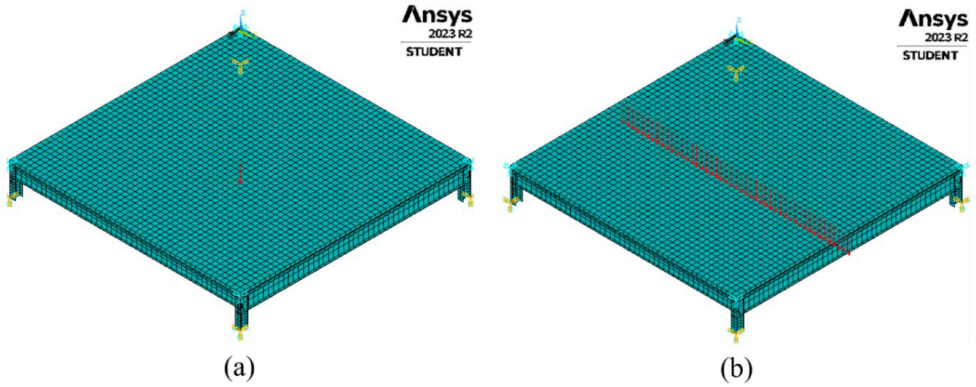

Figure 1. Spatial distribution of the walking load.

For the application of dynamic loads in the second method (Figure 1b), the one-step period (T_p) is equal to $1/f_s$. The contact time at each node is equal to T_p/NN, where NN is the number of nodes in the length of a step (L_{step}), as shown in Figure 2, being d the size of the finite element mesh.

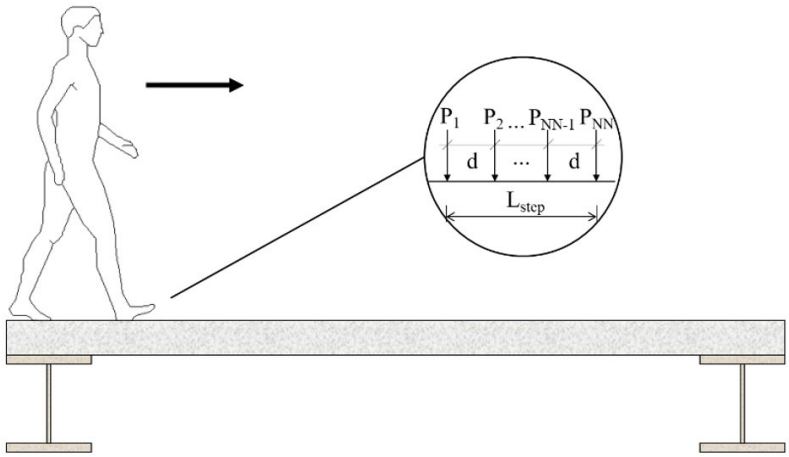

Figure 2. Walking load application [35].

Loads P_1 to P_{NN} were applied separately. The first load was applied from zero to the contact time, and then became zero; the second load was applied for twice the contact time, and subsequently along the walking path. Application of the load in the first case (Figure 1a) adopted the total analysis time of the second case.

2.1.1 Fourier series

The Fourier series is one of the first dynamic models proposed to describe human actions. This model is characterized by the sum of the harmonics (i) according to Equation 1.

$$F(t) = Q[1 + \sum_{i=1}^{n} \alpha_i cos(2\pi i f_s t + \varphi_i)] \quad (1)$$

Table 2 lists some dynamic parameters of human walking [16], [38]. The numerical simulations in this study used the dynamic coefficients proposed by Rainer et al. [16] and the phase angles proposed by Bachmann and Ammann [4], which are equal to $0, \frac{\pi}{2}, \frac{\pi}{2}$.

Table 2. Dynamic coefficients of human walking.

	Rainer et al. [16]	Kerr [38]
1st Harmonic	0.5	$-0.2649f_s^3 + 1.3206f_s^2 - 1.7597f_s + 0.7613$
2nd Harmonic	0.2	0.07
3rd Harmonic	0.1	0.05
4th Harmonic	0.05	0.05
5th Harmonic	—	0.03

According to Ohlsson [18] and Ebrahimpour et al. [20], three harmonics are sufficient to describe human walking. However, Varela and Battista [6] pointed out that the fourth harmonic may be close to the fundamental floor frequency, and cause dynamic response amplification. A Fourier series model was applied using three and four harmonics (F3 and F4). The same model was applied using only temporal variations: static in the center of the walking path (F3S and F4S), and spatial and temporal variations distributed along the walking path (F3D and F4D). Figure 3 shows the dynamic model.

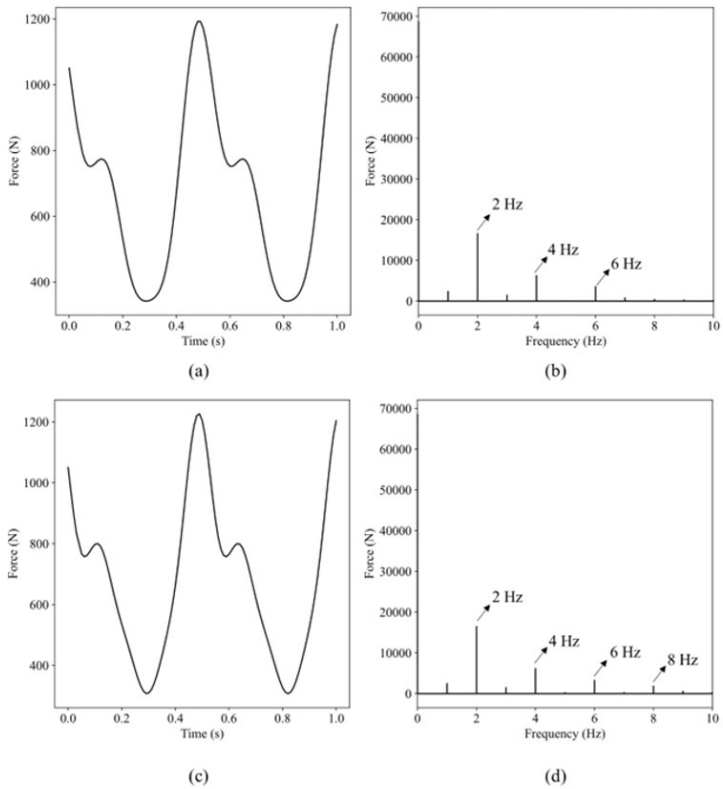

Figure 3. Fourier series load model: three-harmonic time domain (a) and frequency domain (b) and four-harmonic time domain (c) and frequency domain (d).

2.1.2 Single foot force model

The second model was proposed by Li et al. [39], whose purpose was to develop a formulation without the need for phase angles. The model is based on the hypothesis of representing the single foot force (SFF), which is different from other dynamic models that present the superimposition of steps. Equations 2 to 7 represent the dynamic SFF model. The dynamic coefficients vary according to the step frequency used in the experiment.

$$F(t) = Q\sum_{i=1}^{5}\alpha_i sin(\pi i f_s t) \quad (2)$$

$$\alpha_1 = -0.0698 f_s + 1.211, for\ 1.6\ Hz \leq f_s < 2.32\ Hz \quad (3)$$

$$\alpha_2 = 0.1052 f_s - 0.1284, for\ 1.6\ Hz \leq f_s < 2.32\ Hz \quad (4)$$

$$\alpha_3 = 0.3002 f_s - 0.1534, for\ 1.6\ Hz \leq f_s < 2.32\ Hz \quad (5)$$

$$\alpha_4 = 0.0416 f_s - 0.0288, for\ 1.6\ Hz \leq f_s < 2.32\ Hz \quad (6)$$

$$\alpha_5 = -0.0275 f_s + 0.0608, for\ 1.6\ Hz \leq f_s < 2.32\ Hz \quad (7)$$

During the one-step period, there is an instant where both feet are in simultaneous contact with the floor. According to Ebrahimpour et al. [20], this contact period can be considered equal to 24% of the one-step period. Figure 4 illustrates the dynamic model.

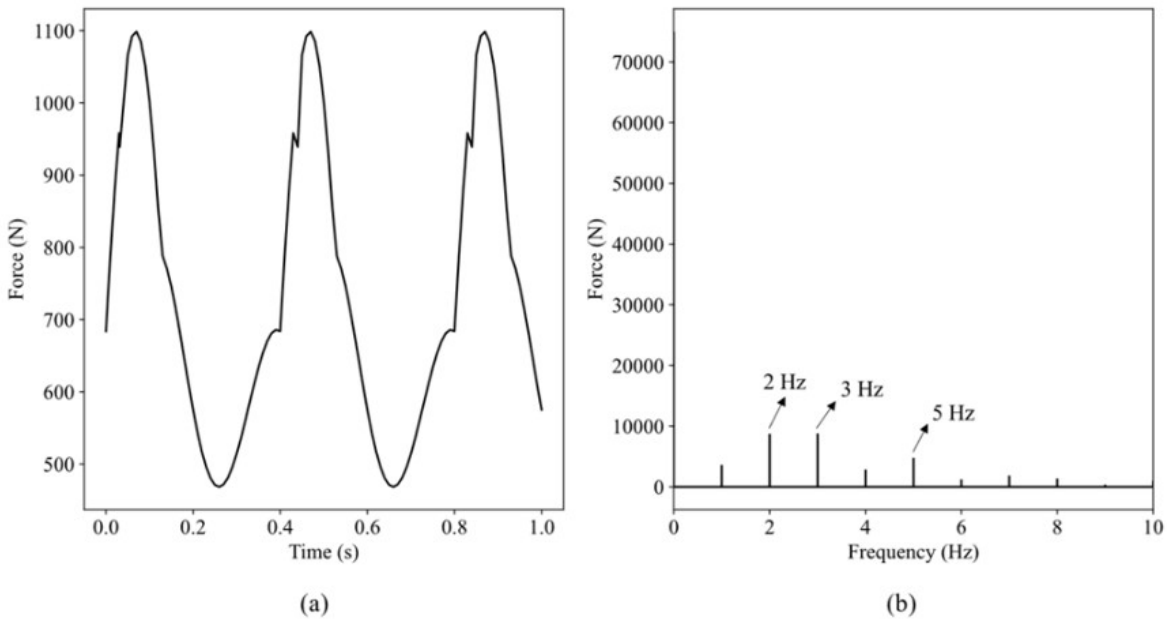

Figure 4. Single foot force load model: time domain (a) and frequency domain (b).

2.1.3 Human Dynamic Model by Varela et al. [40]

Varela et al. [40] conducted an experimental study to determine new dynamic factors for human walking. Equations 8 to 10 define the proposed dynamic coefficients, which vary according to the step frequency of the experiment. The phase angles obtained for the experimental tests were equal to 0º, 85.6°, and 89.4°. The dynamic model proposed by Varela et al. [40], FSV, was applied to Equation 1, as shown in Figure 5.

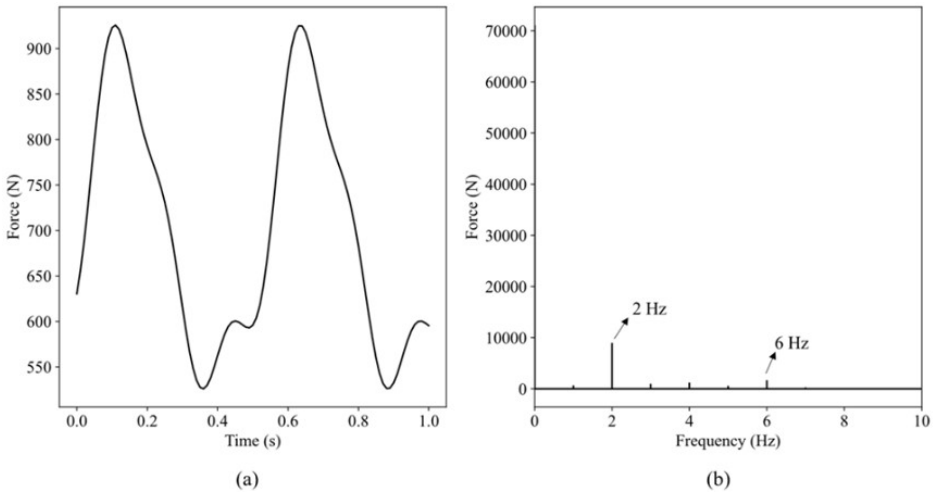

Figure 5. FSV load model: time domain (a) and frequency domain (b).

$$\alpha_1 = 0.1556 f_s^2 - 0.1816 f_s + 0.0356 \tag{8}$$

$$\alpha_2 = \begin{cases} 0.065, for\ f_s \leq 2.0\ Hz \\ 0.1958 f_s - 0.3266, for\ f_s > 2.0\ Hz \end{cases} \tag{9}$$

$$\alpha_3 = 0.054 \tag{10}$$

2.1.4 Biodynamic model

The first dynamic model that represented human walking, considered the body to be a simple source of force. However, in recent years, the number of studies that have analyzed human–structure interaction (HSI) has increased, and it has been observed that the presence of people on floors modified the dynamic response of those structures [41], [42]. The HSI analysis varies according to the adopted approach and considers that the human body can be represented as a model with a single degree of freedom [43] or more than one [44]. For a detailed review, see Roupa et al. [45].

Consequently, biodynamic models have emerged that recognize the human body as a system with mass (m), stiffness (k), and damping (c), which may be obtained through experimental studies.

In this study, the dynamic model proposed by Toso et al. [46] (Bio) was analyzed, as shown in Figure 6. Table 3 lists the biodynamic parameters of the human body obtained through regression analysis.

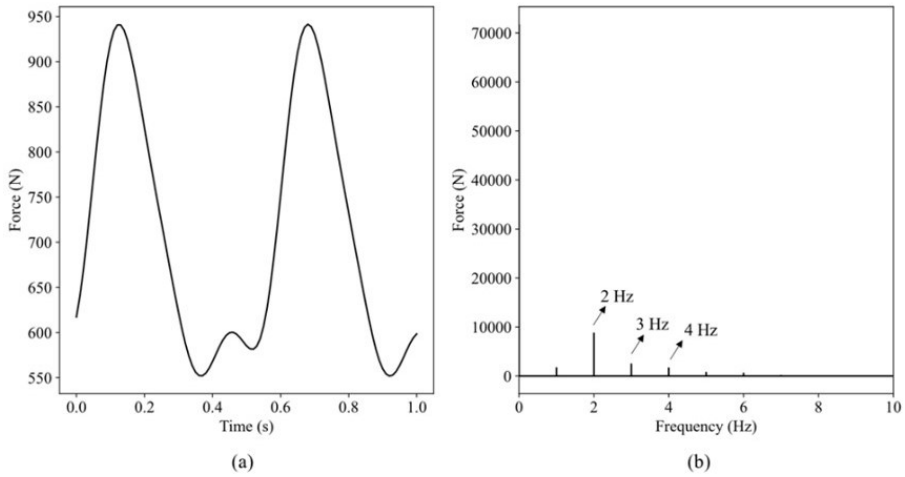

Figure 6. Biodynamic load model: time domain (a) and frequency domain (b).

Table 3. Biodynamic parameters [46].

	m (kg)	c (Ns/m)	k (N/m)
Minimum	11.34	208.99	2544.79
Maximum	106.71	1713.12	18019.79
Average	46.73	577.87	8052.46
Standard deviation	24.49	232.23	3788.02

Toso et al. [46] also proposed three dynamic coefficients, which were based on the biodynamic coefficients, as presented in Equations 11 to 13, where M denotes the mass of the human body. Using these coefficients, the biodynamic model can be applied using Equation 1.

These authors showed that the use of the proposed model with a dynamic coefficient leads to acceleration results that are as good as the biodynamics per se. However, they did not obtain the phase angles for these dynamic coefficients. As a result, the model proposed by Toso et al. [46] was applied in this study using the proposed dynamic coefficients and phase angles defined by Bachmann and Ammann [4], which are equal to $0, \frac{\pi}{2}, \frac{\pi}{2}$.

$$\alpha_1 = 0.22 f_s^2 - 0.45 f_s + 0.35 \tag{11}$$

$$\alpha_2 = 0.0243 + (6.87E-05)c - (1.38E-06)k \tag{12}$$

$$\alpha_3 = -0.0638 + 0.0024M - (1.09E-06)k + (1.0E-08)kM - (1.38E-05)\,M^2 \tag{13}$$

2.1.5 Probabilistic model

According to Brownjohn et al. [19], human walking may be characterized as a non-periodic force, i.e., a random process with a narrow frequency band. Živanović et al. [47] suggested the possibility of energy leakage between the main harmonics and suggested the use of a multiharmonic model. This dynamic model proposes the use of main harmonics and subharmonics. For the main harmonics, the dynamic coefficients α_i were presented by Kerr [38] (Table 2), and for the subharmonics, the dynamic coefficients (α_i^s) are defined in Equations 14 to 18. The phase angles are uniformly distributed in the interval [-π, π], i.e., $-\pi, -\frac{\pi}{2}, 0, \frac{\pi}{2}, \pi$. Equations 19 to 21 provide the probabilistic model (PB) in Figure 7.

$$\alpha_1^s = 0.026\alpha_1 + 0.0031 \tag{14}$$

$$\alpha_2^s = 0.074\alpha_1 + 0.01 \tag{15}$$

$$\alpha_3^s = 0.012\alpha_1 + 0.016 \tag{16}$$

$$\alpha_4^s = 0.013\alpha_1 + 0.0093 \tag{17}$$

$$\alpha_5^s = 0.015\alpha_1 + 0.0072 \tag{18}$$

$$F_i(t) = Q\alpha_i \sum_{f_j=i-0.25}^{i+0.25} \alpha_{n,i}(f_j) \cos\left[2\pi f_j f_s t + \varphi\right] \tag{19}$$

$$F_i^s(t) = Q\alpha_i^s \sum_{f_j^s=i-0.75}^{i-0.25} \alpha_{n,i}^s(f_j^s) \cos\left[2\pi f_j^s f_s t + \varphi\right] \tag{20}$$

$$F(t) = \sum_{i=1}^{5} F_i(t) + \sum_{i=1}^{5} F_i^s(t) \tag{21}$$

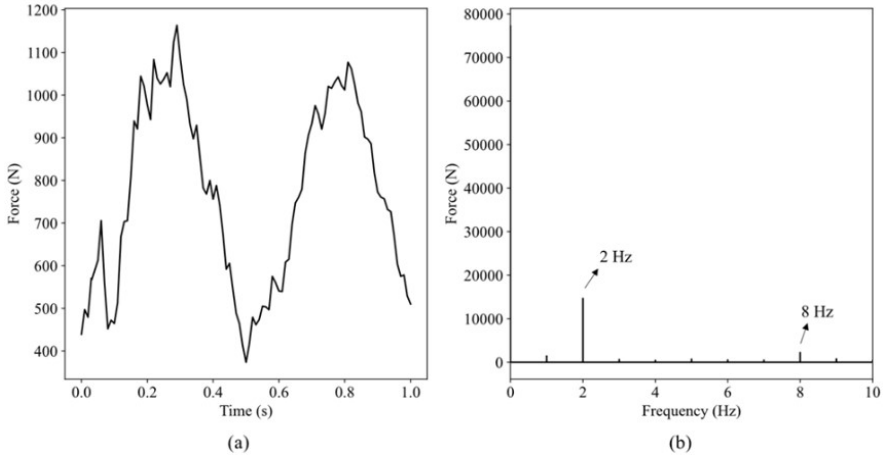

Figure 7. Probabilistic load model: time domain (a) and frequency domain (b).

The subscript "*s*" refers to subharmonics, "*i*" is the number of the harmonic, and f_j is the ratio of the value of the analyzed frequency to the step frequency, which belongs to the interval [*i*-0.25, *i*+0.25) for the harmonics and [*i*-0.75, *i*-0.25) for the subharmonics. $\alpha_{n,i}(f_j)$ and $\alpha^s_{n,i}(f_j^s)$ are the normalized dynamic coefficients for the harmonics and subharmonics, respectively, which can be obtained using Equations 22 and 23 for harmonics and subharmonics, respectively, in as many terms as desired.

$$\alpha_{n,i}(f_j) = a_{i,1}exp\left[-\left(f_j - b_{i,1}\right)/c_{i,1}\right] + a_{i,2}exp\left[-\left(f_j - b_{i,2}\right)/c_{i,2}\right] + a_{i,3}exp\left[-\left(f_j - b_{i,3}\right)/c_{i,3}\right] \quad (22)$$

$$\alpha^s_{n,i}(f_j^s) = a^s_{i,1}exp\left[-\left(f_j^s - b^s_{i,1}\right)/c^s_{i,1}\right] + a^s_{i,2}\, exp\left[-\left(f_j^s - b^s_{i,1}\right)/c^s_{i,1}\right] \quad (23)$$

The coefficients $a_{i,k}$, $b_{i,k}$, $c_{i,k}$ (k = 1, 2, 3) and $a^s_{i,j}$, $b^s_{i,j}$, $c^s_{i,j}$ (j = 1, 2) are listed in Tables 4 and 5, respectively.

Table 4. Dynamic coefficients for the harmonics [47].

i	1	2	3	4	5
$a_{i,1}$	0.7852	0.513	0.3908	0.3255	0.2806
$b_{i,1}$	0.9999	2.00	3.00	4.00	4.999
$c_{i,1}$	0.008314	0.01105	0.00956	0.008797	0.007939
$a_{i,2}$	0.0206	0.133	0.1567	0.1647	0.1584
$b_{i,2}$	1.034	1.957	3.00	4.001	5.004
$c_{i,2}$	0.2524	0.263	0.05525	0.06641	0.07825
$a_{i,3}$	0.1074	-0.04984	0.06866	0.06888	0.07289
$b_{i,3}$	1.001	1.882	2.957	3.991	4.987
$c_{i,3}$	0.03653	0.05807	0.5607	0.375	0.4501

Table 5. Dynamic coefficients for the subharmonics [47].

i	1	2	3	4	5
$a^s_{i,1}$	0.3406	0.3024	0.2627	0.2344	0.2645
$b^s_{i,1}$	0.4988	1.50	2.50	3.501	4.499
$c^s_{i,1}$	0.00834	0.00874	0.00975	0.0099	0.01019
$a^s_{i,2}$	0.2803	0.1345	0.2456	0.2355	0.2389
$b^s_{i,2}$	1.133	1.532	0.2312	-1.576	1.153
$c^s_{i,2}$	0.6388	0.7233	2.932	7.05	4.561

2.1.6 Heel impact model

Generally, smooth sinusoidal equations represent human walking; however, by conducting experimental tests, it was possible to observe peaks of force at the beginning of each step [19], [34]. These peaks occurred when the heel impacted the floor. Varela and Battista [6] proposed the use of a dynamic model that includes the effects of heel impact (HI), given by Equations 24 to 28.

$$F_1(t) = (f_{mi}F_m - Q)t/0.04T_p + Q \tag{24}$$

$$F_2(t) = f_{mi}F_m\left[C_1\left(t - 0.04T_p\right)/0.02T_p\ + 1\right] \tag{25}$$

$$F_3(t) = F_m \tag{26}$$

$$F_4(t) = Q\left\{1 + \sum_{i=1}^{n}\alpha_i \sin\left[2\pi i f_s\left(t + 0.1T_p\right) - \varphi_i\right]\right\} \tag{27}$$

$$F_5(t) = 10(Q - C_2)\left(t/T_p - \ 1\right) + Q \tag{28}$$

F_m is the maximum value of the Fourier series given by Equation 29, f_{mi} is the increasing factor that considers the heel impact, and C_1 and C_2 are coefficients determined using Equations 30 and 31, where n is the number of adopted harmonics.

$$F_m = 1 + \sum_{i=1}^{n}\alpha_i \tag{29}$$

$$C_1 = (1/f_{mi} - 1) \tag{30}$$

$$C_2 = \begin{cases} Q(1-\alpha_2), for\ n = 3 \\ Q(1-\alpha_2-\alpha_4), for\ n = 4 \end{cases} \tag{31}$$

Varela and Battista [6] indicated that the value of f_{mi} varies among people and shoe types. In the present study, the increasing factor f_{mi} was assumed to be equal to 1.12 and 1.25. The dynamic coefficients were defined by Rainer et al. [16] (Table 2) and the phase angles were equal to $0, \frac{\pi}{2}, \pi, \frac{3\pi}{2}$. Figure 8 illustrates the dynamic model.

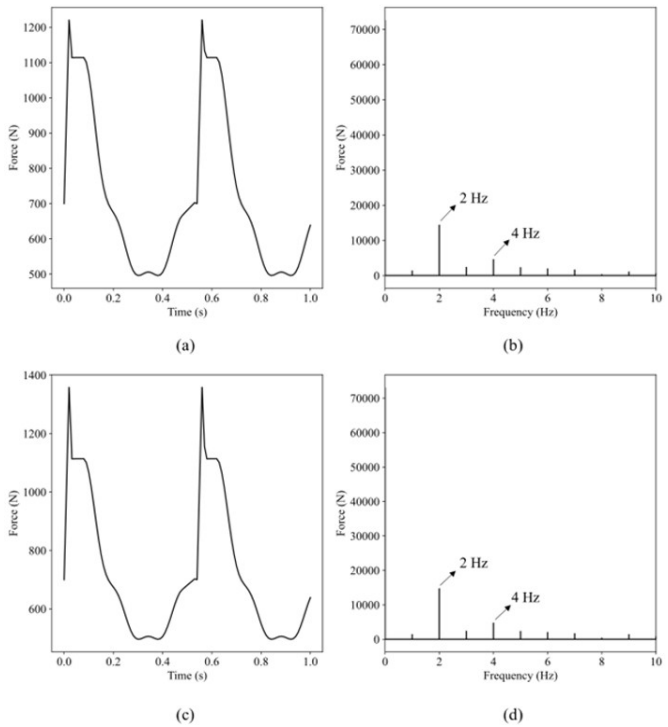

Figure 8. Heel Impact load model: f_{mi} = 1.12-time domain (a) and frequency domain (b) and f_{mi} = 1.25-time domain (c) and frequency domain (d).

2.1.7 Comparison of the dynamic models

Various dynamic models that describe human walking loading have been described in the literature. Based on a set of experimental results, the goal of the present study is to verify which dynamic models yield results that are closer to the experimental results. Table 6 presents the maximum values of the dynamic models. In comparison to the Fourier series with three harmonics (F3), the maximum load values with the biodynamic model [46] and the model proposed by Varela et al. [40] were approximately 78.8% and 77.48%, respectively, whereas that for the Heel Impact model [6] was 102.14% and 113.65% for the f_{mi} equal to 1.12 and 1.25, respectively. Table 6 presents other percentage comparison values.

Dynamic models were applied separately to the computational floor models, as described in Section 2.3.

Table 6. Maximum forces for the dynamic load models

Model	Maximum force (N)	Percentage ratio
F3	1194.71	1.0
F4	1227.53	1.0275
SFF	1098.68	0.9196
FSV	925.71	0.7748
Bio	941.43	0.788
PB	1163.66	0.974
HI1.12	1220.23	1.0214
HI1.25	1357.81	1.1365

2.2 Tested composite steel and concrete floors

Four composite steel and concrete floors were experimentally tested by other researchers, and all documented results available were considered for analysis. Among these floors, two were classified as having a low fundamental frequency, and two as having a high fundamental frequency. The analyses of all four floors generated fundamental frequency and acceleration results, either peak or root mean square (RMS) acceleration.

2.2.1 Long span composite slab laboratory specimen

The first floor, which consisted of a laboratory specimen with dimensions of 9.15 m × 9.15 m, was tested by Davis [30]. The floor system was built with 222 mm thick normal-weight concrete on a 117.5 mm high steel deck, supported by welded steel beams. The longitudinal elastic modulus of the concrete, PM, and Poisson's ratio were 50 GPa, 5.00, and 0.2, respectively. The details of the beams used and their spacing are shown in Figure 9a, and the columns were modeled using W12 × 40.

Walking tests were performed in the direction of the ribs (walking path 1) and perpendicular to the ribs (walking path 2), and the acceleration results were obtained at the center of the floor (point P1), as shown in Figure 9b. Walking tests were performed with only one male person between 25 and 40 years of age and in good health. Davis [30] did not report the weight of the walkers. The walking tests were performed at a step frequency of 1.67 Hz and the damping coefficient was experimentally estimated to be 0.436%.

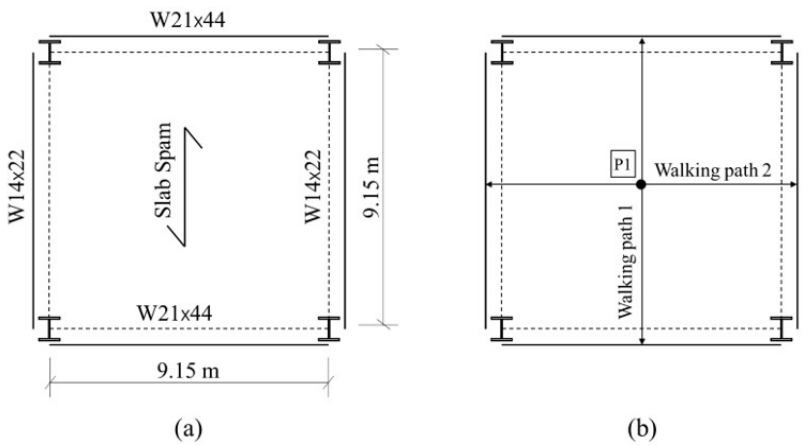

Figure 9. Structural plan of the first floor (a) and walking test information (b).

2.2.2 Full-scale composite floor

The second floor, which was located in a building to be built in Kuwait, was tested by Fahmy and Sidky [28] in a case study. The floor had dimensions of 18.2 m × 9.0 m, with welded beams and a normal-weight concrete slab with 120 mm thickness. Figure 10a shows the details of the beams used and the floor layout. The longitudinal elastic modulus of the concrete and the Poisson's ratio were 36.17 GPa and 0.2, respectively.

The walking tests were performed in the longitudinal direction of the floor, as presented in Figure 10b, with only one male person, in good health, weighing approximately 75 kg. The acceleration results were obtained at ten different points: four on the walking path and six outside the walking path, as shown in Figure 10b. The tests were performed at a step frequency of 2.2 Hz and the damping coefficient was estimated to be 1.3%.

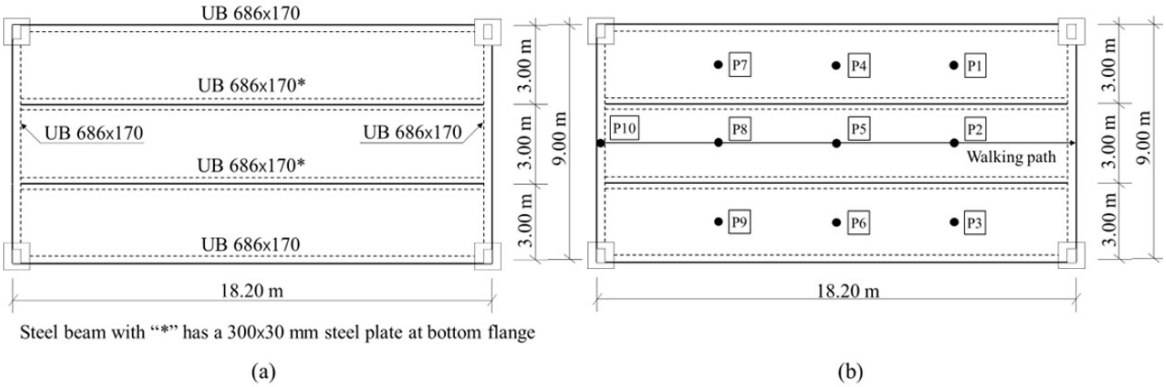

Figure 10. Second floor structural plan (a) and walking test information (b).

2.2.3 University Classroom 403

The third floor, which consisted of a classroom at the College of Health Science, University of Kentucky, was tested by Liu and Davis [31]. The floor dimensions were 20.0 m × 11.3 m and it was built of a 150 mm thick normal-weight concrete slab on a 50 mm thick steel deck supported by steel beams; details are shown in Figure 11a. The longitudinal elastic modulus of the concrete, PM, and Poisson's ratio were 31.7 GPa, 1.50, and 0.2, respectively.

Walking tests were performed with only one male participant weighing 61.23–65.77 kg. These tests were made along the walking path at bay F1 and the acceleration results were obtained at point P1, as shown in Figure 11b. Walking tests were performed at five different step frequencies: 1.5, 1.67, 1.83, 2.0, and 2.17 Hz. Liu and Davis [31] did not document the structural damping coefficient; therefore, a value of 3% was used in the present study, following the recommendations of Murray et al. [7]. These authors also indicated the need to include elements to represent the partitions, with a stiffness of 2.15 x 10^3 kN/m/m at the positions shown in Figure 11b.

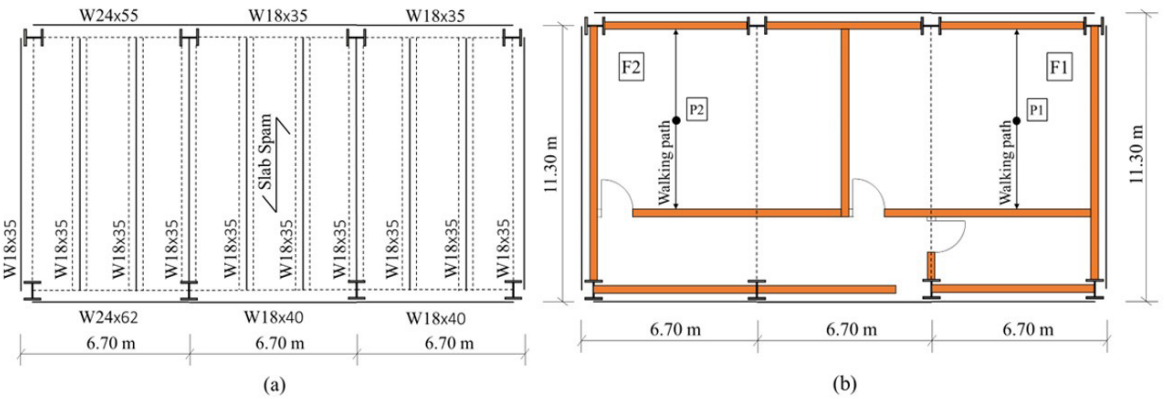

Figure 11. Third floor structural plan (a) and architectural plan, with walking test information (b).

2.2.4 University Classroom 405

The fourth floor, which was located in another room on the fourth floor of the College of Health Science, was also tested by Liu and Davis [31]. All the dimensions and physical and dynamic properties of this floor were identical to those of the third tested floor in classroom 403.

The walking tests for this floor were made on the walking path at bay F2 and the acceleration results were obtained at point P2, as shown in Figure 11b. Similar to the third floor tested, the tests were performed with only one male person by time, weighing 61.23–65.77 kg, and the walking tests were performed with five different step frequencies:1.67, 1.83, 2.0, 2.08, and 2.17 Hz.

2.3 Computational models

All the composite steel and concrete floors were modeled using ANSYS [48], where the SHELL181 element was used to model the slabs and the BEAM188 element was used to model the beams and columns. For the steel deck slabs, the procedure proposed by Barrett [29] was used to define the concrete as an orthotropic material. The nonstructural elements, such as the partitions, were modeled with the COMBIN14 spring element, whose stiffness value was equal to that suggested by Liu and Davis [31]. The offset of the steel beams from the slab edge was also considered in the numerical model. Structural damping was added to the models using the Rayleigh damping matrix [49]. If the floor did not have information regarding this coefficient, the value adopted was based on the suggestions of Murray et al. [7]. For the human dynamic load models, the documented walker weight was used; if this value was not known, a value of 700 N was adopted.

Modal, harmonic, and transient analyses were conducted on each floor. The first analysis was performed using the Block Lanczos method to obtain the natural frequencies and the mode shapes normalized to the mass matrix. The second analysis was designed to obtain the floor frequency domain (i.e., the amplitude of the dynamic results, according to the external frequency) and the solution method was defined as “full”. Finally, a transient analysis was performed on each floor for each dynamic load model. The step frequencies of the dynamic models were equal to those obtained during the experiments. The purpose of this analysis was to obtain an accelerogram of the floor for each dynamic model in the time domain, which was directly compared with the experimental results. Full analysis was adopted as the solution method. For the solution controls, a small displacement analysis was performed with an integration interval of 0.001 s. This integration interval was defined based on the recommendations of Mello et al. [35], considering that the contact time of each load at each node (Figure 2) was higher than this value. The Newmark algorithm was selected as the time integration option, and the equation solvers were defined using this program.

In total, 130 transient simulations were performed for all composite floors, which yielded 220 acceleration histories.

2.3.1 Long span composite slab laboratory specimen

The computational model of the first floor (Figure 12a) was created using 2348 finite elements and 2257 nodes, and resulted in 13506 degrees of freedom. The same regular meshes were adopted for the beams and slabs to guarantee the interactions among these elements. Figure 12b shows the results of the harmonic analysis. It should be noted that the frequency that caused a higher response is 4.4 Hz, which is close to the third harmonic of the exciting load.

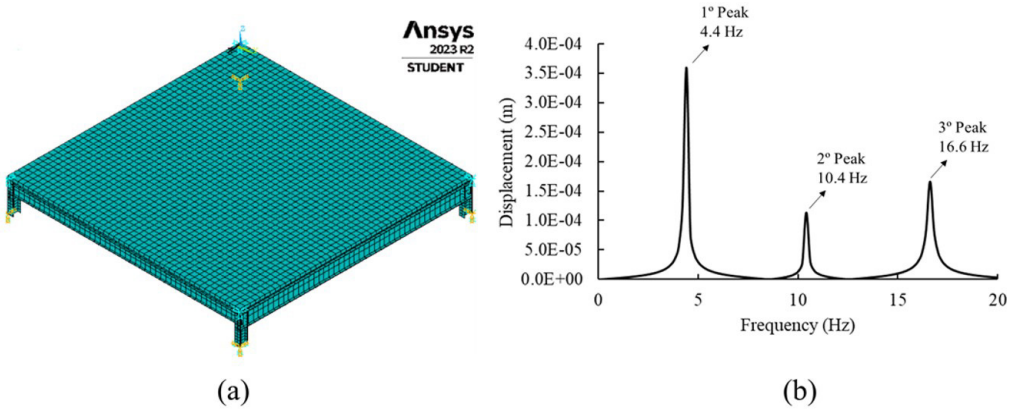

Figure 12. Numerical model (a) and harmonic response (b) for the first floor.

2.3.2 Full-scale composite floor

The second floor model used 2992 finite elements and 2738 nodes, and resulted in 16416 degrees of freedom (Figure 13a). Similar to the first example, this is defined as a regular mesh. The results of harmonic analysis are shown in Figure 13b. It should be noted that the frequency that caused a higher response is 4.8 Hz, which is close to the second harmonic of the exciting load.

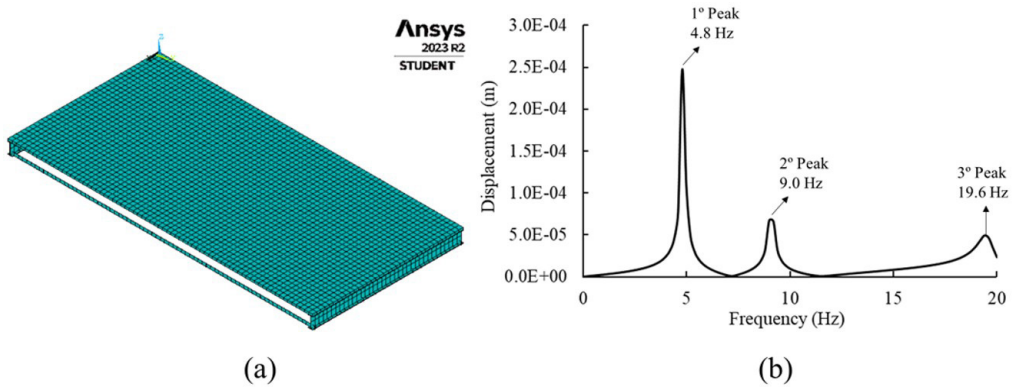

Figure 13. Numerical model (a) and harmonic response (b) for the second floor.

2.3.3 University classrooms

The computational models of the third and fourth floors had 5258 finite elements and 4776 nodes, and resulted in 24356 degrees of freedom (Figure 14a). Regular meshes and spring elements were used to model the partitions. Figures 14b and c show the results of the harmonic analysis. It should be noted that the frequency that caused a higher response is 11.2 Hz for both floors. Moreover, as expected for floors with a high fundamental frequency, the other frequencies have less influence on the floor response than the fundamental frequency.

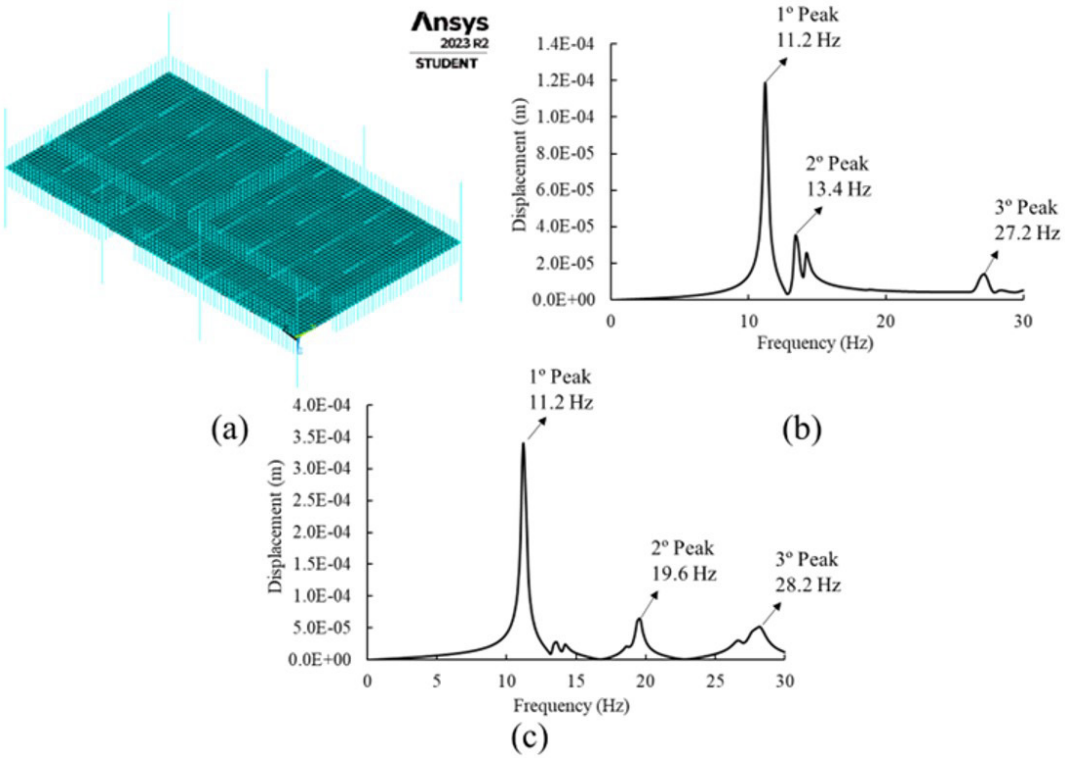

Figure 14. Numerical model (a) and harmonic response for the third (b) and fourth floor (c).

3 RESULTS AND DISCUSSION

This section presents the modal and transient analyses of four composite steel and concrete floors under the dynamic load model. As a reminder, these dynamic models and their nomenclatures are presented in Table 7.

Table 7. Dynamic load model nomenclature.

Dynamic load model	Nomenclature
Fourier series with 3 harmonics and load in one point	F3S
Fourier series with 3 harmonics and load distributed along the walking path	F3D
Fourier series with 4 harmonics and load in one point	F4S
Fourier series with 4 harmonics and load distributed along the walking path	F4D
Biodynamic model proposed by Toso et al. [46]	Bio
Human walking model proposed by Varela et al. [40]	FSV
Probabilistic model [47]	PB
Single foot force model [39]	SFF
Heel Impact model with f_{mi} = 1.12 [7]	HI1.12
Heel Impact model with f_{mi} = 1.25 [7]	HI1.25

3.1 Floors with a low fundamental frequency

3.1.1 Long span composite slab laboratory specimen

Modal analysis was performed, and the natural frequencies and mode shapes are listed in Table 8. According to Davis [30], the fundamental frequency of the floor (after the experimental analysis) was 4.98 Hz and a predominance of the flexion mode shape was observed in the numerical model. After numerical modeling in the present study, a fundamental frequency of 4.35 Hz was obtained using the exact properties described by Davis [30]. The difference in the fundamental frequency was 0.63 Hz. Because the results agreed with the reference experimental and numerical models, it was considered admissible to verify the vibration conditions.

Table 8. Natural frequencies and mode shapes of the first floor.

	Frequency (Hz)	Mode Shape
1	4.3508	Flexion
2	7.4082	Flexion
3	10.188	Flexion
4	10.406	Flexion
5	15.872	Flexion

The transient analysis yielded acceleration results for all the load models in the two floor directions (Figure 9b). Davis [30] obtained a peak acceleration and RMS of 1.36%g and 0.541%g, respectively, for direction 1, and 0.972%g and 0.404%g, respectively, for direction 2. Table 9 presents the numerical results for all dynamic models and the errors for the peak (a_p error) and RMS (a_{rms} error) accelerations compared with the experimental values.

The peak acceleration results showed that except for the Fourier series model applied to the center of the walking path (F3S and F4S), all models yielded values above the experimental results. It can also be observed that the number of harmonics used for the Fourier series did not cause a significant difference in the dynamic response of the floor, with an average difference of approximately 0.04%g. This can be explained by less influence of this frequency on the floor response (Figure 12b).

Table 9. Results for the first floor.

Load Model	Parallel to the ribs				Perpendicular to the ribs			
	a_p (%g)	a_{rms} (%g)	a_p error (%g)	a_{rms} error (%g)	a_p (%g)	a_{rms} (%g)	a_p error (%g)	a_{rms} error (%g)
Experimental results	1.36	0.541	—	—	0.972	0.404	—	—
F3S	0.920	0.257	-0.440	-0.284	0.920	0.257	-0.052	-0.147
F3D	1.716	0.205	0.356	-0.336	1.538	0.219	0.566	-0.185
F4S	0.922	0.258	-0.438	-0.283	0.922	0.258	-0.050	-0.146
F4D	1.677	0.205	0.317	-0.336	1.580	0.220	0.608	-0.184
Bio	1.394	0.135	0.034	-0.406	1.213	0.158	0.241	-0.246
FSV	1.601	0.261	0.241	-0.280	1.320	0.264	0.348	-0.140
PB	1.752	0.279	0.392	-0.262	1.462	0.210	0.490	-0.194
SFF	2.216	0.813	0.856	0.272	1.828	0.499	0.856	0.095
HI1.12	2.855	0.778	1.495	0.237	2.038	0.655	1.066	0.251
HI1.25	4.584	1.085	3.224	0.544	3.565	1.448	2.593	1.044

The biodynamic model [46] provided the results with the lowest errors for peak acceleration for both directions, followed by the model proposed by Varela et al. [40]. The peak acceleration results for these models were similar, as the percentage ratio of the maximum force. The Heel Impact model [6] had the highest errors in peak acceleration because its maximum load was also the highest (Table 6).

For the RMS acceleration results, the Heel Impact model [6] with f_{mi} = 1.12, had the lowest errors, close to the single foot force [39], in the direction parallel to the ribs, both in favor of security. In the perpendicular direction, the single foot force [39] had the lowest errors.

The other dynamic models achieved RMS accelerations below the experimental values, with errors between -0.14%g and -0.41%g. The biodynamic model [46] had the worst results in the RMS acceleration analysis, and, therefore, may be uncomfortable for humans.

3.1.2 Full-scale composite floor

In their experimental campaign using the heel drop test, Fahmy and Sidky [28] achieved a fundamental floor frequency of 4.38 Hz. The authors did not perform a numerical analysis to define the floor mode shape. A modal analysis of this floor was performed, and the natural frequencies and mode shapes are presented in Table 10. When comparing only the fundamental frequency, an absolute error of 0.46 Hz can be noted. The experimental results yielded a fundamental frequency close to the second harmonic of the step frequency. The numerical model remained close to the range of the second harmonic and was quite close to the third harmonic. At both points, these frequencies caused reasonable floor responses (Figure 12b). Therefore, because the numerical results were close to the reference values, this floor was considered acceptable for verifying vibration conditions.

Table 10. Natural frequencies and mode shapes of the second floor.

	Frequency (Hz)	Mode Shape
1	4.8435	Flexure
2	6.4334	Flexure
3	9.0991	Flexure
4	12.297	Flexure
5	14.6	Flexure

Transient analyses were performed with all the dynamic models in the walking path, and peak acceleration results at 10 selected points were obtained (Figure 10b). Fahmy and Sidky [28] obtained peak acceleration results of 2.867, 4.347, 2.677, 4.000, 5.18, 3.58, 2.743, 3.987, 2.640, and 1.563%g, respectively for the 10 points. The numerical results and their errors compared with the experimental values for all points are presented in Tables 11 and 12, respectively.

Table 11. Results of points 1 to 5 on the second floor.

Load Model	Point 01		Point 02		Point 03		Point 04		Point 05	
	a_p (%g)	a_p error (%g)	a_p (%g)	a_p error (%g)	a_p (%g)	a_p error (%g)	a_p (%g)	a_p error (%g)	a_p (%g)	a_p error (%g)
Experimental results	2.867	—	4.347	—	2.677	—	4.000	—	5.180	—
F3S	0.508	-2.359	0.677	-3.670	0.457	-2.220	0.560	-3.440	1.766	-3.414
F3D	0.576	-2.291	4.357	0.010	0.538	-2.139	0.448	-3.552	4.437	-0.743
F4S	0.509	-2.358	1.103	-3.244	0.580	-2.097	0.633	-3.367	1.866	-3.314
F4D	0.539	-2.328	4.934	0.587	0.520	-2.157	0.415	-3.585	4.392	-0.788
Bio	0.418	-2.449	4.172	-0.175	0.437	-2.240	0.389	-3.611	3.978	-1.202
FSV	0.491	-2.376	4.482	0.135	0.454	-2.223	0.449	-3.551	4.580	-0.600
PB	0.611	-2.256	4.315	-0.032	0.592	-2.085	0.619	-3.381	4.523	-0.657
SFF	0.837	-2.030	4.463	0.116	0.765	-1.912	0.880	-3.120	4.498	-0.682
HI1.12	1.082	-1.785	5.268	0.921	1.196	-1.481	1.103	-2.897	4.960	-0.220
HI1.25	1.242	-1.625	5.967	1.620	1.523	-1.154	1.216	-2.784	5.508	0.328

Table 12. Results of points 6 to 10 on the second floor.

Load Model	Point 06		Point 07		Point 08		Point 09		Point 10	
	a_p (%g)	a_p error (%g)	a_p (%g)	a_p error (%g)	a_p (%g)	a_p error (%g)	a_p (%g)	a_p error (%g)	a_p (%g)	a_p error (%g)
Experimental results	3.580	—	2.743	—	3.987	—	2.640	—	1.563	—
F3S	0.605	-2.975	0.402	-2.341	0.806	-3.181	0.402	-2.238	0.516	-1.047
F3D	0.453	-3.127	0.543	-2.200	3.575	-0.412	0.541	-2.099	2.212	0.649
F4S	0.622	-2.958	0.526	-2.217	0.862	-3.125	0.526	-2.114	0.800	-0.763
F4D	0.446	-3.134	0.550	-2.193	4.820	0.833	0.550	-2.090	2.237	0.674
Bio	0.421	-3.159	0.445	-2.298	3.681	-0.306	0.464	-2.176	1.871	0.308
FSV	0.378	-3.202	0.446	-2.297	4.586	0.599	0.446	-2.194	1.912	0.349
PB	0.572	-3.008	0.556	-2.187	4.287	0.300	0.630	-2.010	2.043	0.480
SFF	0.706	-2.874	0.678	-2.065	4.769	0.782	0.656	-1.984	1.982	0.419
HI1.12	1.161	-2.419	0.918	-1.825	4.724	0.737	0.822	-1.818	1.865	0.302
HI1.25	1.270	-2.310	1.165	-1.578	4.869	0.882	0.985	-1.655	1.939	0.376

The peak acceleration results for this floor can be split into two samples: points on the walking path (2, 5, 8, and 10) and points outside the walking path (1, 3, 4, 6, 7, and 9), as shown in Figure 10b.

For the points on the walking path, the Fourier series applied at one point (F3S and F4S) yielded the highest errors, confirming the need to consider the entire walking path. The acceleration results for the other dynamic models were similar to those in the experimental references. The biodynamic model [46] proposed by Varela et al. [40] and the Fourier series presented the lowest errors.

For the points outside the walking path, all models presented peak acceleration values that were significantly lower than the experimental values. The errors reached values of –3.611%g (biodynamic model [46] at point 4), which may be uncomfortable for humans [7]. These high error values may be explained by the typical formulation of a dynamic model. In general, the dynamic models were calibrated by considering the results of the walking path. Therefore, to analyze the vibration results in adjacent bays, it is necessary to consider appropriate dynamic models. The dynamic model that presented the lowest errors for the points outside the walking path was the Heel Impact model with f_{mi} = 1.25, because its maximum load was the highest (Table 6).

3.2 Floors with a high fundamental frequency

3.2.1 University Classroom 403

Liu and Davis [31] used heel-drop tests to determine a fundamental classroom frequency of 10.65 Hz. These authors also developed a numerical model of this floor, initially without including the partitions and then adding them. For both cases, they ran a modal analysis to validate the floor, and reached fundamental frequencies of 6.33 Hz and 10.56 Hz, respectively, with the predominance of flexural mode shapes. In this study, two modal analyses were performed for this floor: first, without partitions, and after adding them, with the stiffness suggested by Liu and Davis [31]. For the first analysis, the fundamental frequency was equal to 6.65 Hz. For the second analysis, the natural frequencies and mode shapes are presented in Table 13. Based on the reference values presented by Liu and Davis [31], it is possible to observe that the fundamental frequencies are similar, and that absolute errors, for the cases without and with the partitions, were equal to 0.32 Hz and 0.54 Hz, respectively. Moreover, the mode shapes agree with the reference mode shapes. Because the range of the numerical results was close to the reference values, this floor was considered acceptable for verifying the vibration conditions.

Table 13. Natural frequencies and mode shapes for the third and fourth floors.

	Frequency (Hz)	Mode Shape
1	11.19	Flexion
2	11.291	Flexion
3	13.458	Flexion
4	14.17	Flexion
5	14.377	Flexion

Similar to the second floor, only the peak acceleration experimental results were available for the five step frequencies for which the floor was experimentally tested: 0.279, 0.357, 0.397, 0.445, and 0.653%g, respectively. Transient analyses were performed for five step frequencies along the walking path, and the peak acceleration results were obtained at the central point of the walking path (Figure 11b). Table 14 shows a comparison of the numerical results and their errors.

Table 14. Results for the third floor.

Load Model	f_s = 1.50 Hz		f_s = 1.67 Hz		f_s = 1.83 Hz		f_s = 2.0 Hz		f_s = 2.17 Hz	
	a_p (%g)	a_p error (%g)	a_p (%g)	a_p error (%g)	a_p (%g)	a_p error (%g)	a_p (%g)	a_p error (%g)	a_p (%g)	a_p error (%g)
Experimental results	0.279	—	0.357	—	0.397	—	0.445	—	0.653	—
F3S	0.845	0.566	0.907	0.550	0.907	0.510	1.006	0.561	1.106	0.453
F3D	0.598	0.319	0.529	0.172	0.609	0.213	0.598	0.153	0.906	0.254
F4S	0.906	0.627	0.919	0.562	0.911	0.515	1.164	0.719	1.237	0.584
F4D	0.657	0.378	0.569	0.212	0.632	0.235	0.624	0.179	0.931	0.278
Bio	0.461	0.182	0.409	0.052	0.499	0.102	0.458	0.013	0.718	0.065
FSV	0.472	0.193	0.433	0.076	0.508	0.111	0.465	0.020	0.696	0.043
PB	0.795	0.516	0.610	0.253	0.707	0.311	0.635	0.190	0.994	0.341
SFF	0.795	0.516	0.622	0.265	0.756	0.360	0.653	0.208	1.051	0.398
HI1.12	1.122	0.843	1.177	0.820	1.208	0.812	1.111	0.666	1.373	0.720
HI1.25	1.233	0.954	1.417	1.060	1.273	0.876	1.252	0.807	1.508	0.856

Based on these results, it can be confirmed that using a Fourier series with a load applied at only one point is not recommended, because peak accelerations higher than three times the reference values are reached. The Fourier series using four harmonics and moving along the walking path did not elicit a significant response compared to the same model using three harmonics for any step frequency used. This situation may be explained by the fact that the frequency with the highest response was 11.2 Hz (Figure 14b) and the 4th harmonic for the highest step frequency was 8.68 Hz; thus, the increase in the acceleration response was not significant. Another reason for the insignificant influence in the response is the combination of the damping ratio and the natural response of a high fundamental frequency, which does not induce resonance.

The biodynamic model [46] and the model presented by Varela et al. [40] provided results that are closest to the experimental results, in which errors decreased as the step frequency increased, and average error values of 0.083%g and 0.089%g, respectively, were reached. Similar to the first two floors, the Heel Impact model had the highest errors in peak acceleration, which may be a result of the maximum load compared with the other dynamic models.

3.2.2 University Classroom 405

Liu and Davis [31] experimentally tested this floor, whose geometry and properties were the same as the third floor. Using the heel drop test, these authors achieved a fundamental frequency of 9.8 Hz and, similar to the third floor, also conducted a numerical simulation that achieved a fundamental frequency of 10.19 Hz, with predominant flexion effects in the mode shapes. In the present study, because the floor is similar to the third floor, the same numerical model was adopted using the exact properties described by Liu and Davis [31], and a fundamental frequency of 11.19 Hz was achieved (Table 13). The difference in the fundamental frequency was 1.0 Hz and 1.39 Hz, compared to the numerical and experimental results, respectively. This difference may be explained by the occupation of the floors modifying the dynamic response [41], [42], which has not been documented, or even by small differences in the physical properties of the materials. Although the analysis in this study is focused on human walking activities and the natural response of floors with a high fundamental frequency is not to induce resonance, this floor was considered acceptable for verifying the vibration conditions.

The peak acceleration results for the five step frequencies for which the floor was experimentally tested were presented by Liu and Davis [31]: 0.266, 0.338, 0.340, 0.241, and 0.332%g, respectively. Transient analyses were performed in this study for the five step frequencies, for all dynamic models along the walking path, and the peak acceleration results at the central point of the walking path (Figure 11b) were obtained. These results are presented in Table 15 along with the errors, compared to the experimental results.

The analysis of the peak acceleration results was similar to that obtained for classroom 403, which corroborates the analysis of floors with a high fundamental frequency. The biodynamic model [46] and the model proposed by Varela et al. [40] had low errors. The Fourier series model also showed reasonable results, but only for load applications with temporal and spatial variations, and step frequencies lower than 2.0 Hz. The use of four harmonics in the Fourier

series led to conclusions similar to those for the third floor, because the fourth harmonic for the highest step frequency was 8.68 Hz, and for this frequency, the increase in the acceleration results is not significant.

Table 15. Results for the fourth floor.

Load Model	f_s = 1.67 Hz		f_s = 1.83 Hz		f_s = 2.00 Hz		f_s = 2.08 Hz		f_s = 2.17 Hz	
	a_p (%g)	a_p error (%g)	a_p (%g)	a_p error (%g)	a_p (%g)	a_p error (%g)	a_p (%g)	a_p error (%g)	a_p (%g)	a_p error (%g)
Experimental results	0.266	—	0.338	—	0.340	—	0.241	—	0.332	—
F3S	0.743	0.478	0.968	0.630	1.023	0.683	1.073	0.832	1.264	0.932
F3D	0.598	0.333	0.553	0.215	0.592	0.252	0.767	0.526	0.608	0.276
F4S	0.762	0.496	1.050	0.712	1.086	0.746	1.202	0.961	1.392	1.060
F4D	0.604	0.339	0.588	0.250	0.621	0.280	0.763	0.522	0.639	0.307
Bio	0.432	0.166	0.400	0.062	0.471	0.131	0.594	0.353	0.536	0.204
FSV	0.450	0.184	0.425	0.088	0.482	0.142	0.602	0.361	0.551	0.219
PB	0.749	0.484	0.572	0.234	0.694	0.354	0.779	0.538	0.907	0.575
SFF	0.742	0.476	0.573	0.236	0.653	0.312	0.762	0.521	1.058	0.726
HI1.12	1.158	0.892	1.051	0.713	1.032	0.691	1.239	0.998	1.441	1.110
HI1.25	1.338	1.072	1.260	0.922	1.251	0.910	1.416	1.175	1.582	1.250

3.3 Statistical analysis

The analyses presented in the previous sections verified the quality of the acceleration results for each analyzed point. To summarize the acceleration results presented in sections 3.1 and 3.2, a set of statistical analyses was developed, including the percent bias parameter (PBIAS), root mean squared error (RMSE), the normality of the samples and then the mean test. The acceleration results were split into two samples: all RMS acceleration results and all peak acceleration results for cases where the measured point was on the walking path.

First, the bias was verified using the PBIAS test and the cumulative errors were determined using the RMSE, according to Equations 32 and 33, respectively. The results of these tests for the two samples for all dynamic models are presented in Table 16.

$$PBIAS = \frac{\sum_{i=1}^{n}(y_i - \hat{y}_i)}{\sum_{i=1}^{n} y_i} \tag{32}$$

$$RMSE = \sqrt{\frac{1}{n}\sum_{i=1}^{n}(\hat{y}_i - y_i)^2} \tag{33}$$

where y_i is the experimental reference value; $\hat{y}_i$ is the numerical values obtained in Tables 9, 11, 12, 14, and 15; and n is the sample size.

Table 16. PBIAS and RMSE results.

	a_{rms}		a_p	
	PBIAS	**RMSE**	**PBIAS**	**RMSE**
F3S	-45.53%	22.58%	-28.77%	159.29%
F3D	-55.15%	27.13%	16.09%	38.95%
F4S	-45.47%	22.55%	-20.28%	152.56%
F4D	-55.09%	27.11%	26.74%	47.16%
Bio	-69.05%	33.60%	1.18%	35.26%
FSV	-44.52%	22.17%	12.88%	28.89%
PB	-48.27%	23.06%	24.47%	41.54%
SFF	38.88%	20.39%	31.73%	53.02%
HI1.12	51.73%	24.45%	64.47%	86.30%
HI1.25	168.01%	83.23%	97.00%	138.59%

As can be noted from the RMS acceleration results, most models had similar values for the PBIAS and RMSE parameters. The model with values closer to the experimental references was the single foot force model [39], whereas the biodynamic model [46] had the second highest PBIAS and RMSE values. Regarding the peak acceleration results, the biodynamic model [46] had the lowest PBIAS value of 1.18%, whereas the model proposed by Varela et al. [40] had the lowest RMSE value of 28.89%. As expected, the Fourier series models with one single point load and the Heel Impact model [6] with f_{mi} = 1.25, presented the worst results, with RMSE parameters above 100%.

Verifying the hypothesis that the results of the dynamic models were statistically equal to the experimental results also allowed us to summarize the developed analysis. Because of the sample size, this analysis was performed only for peak acceleration results. In addition, because F3S, F4S, and HI1.25 presented high PBIAS and RMSE parameter values, these models were not tested.

For the hypothesis tests, a level of significance (α) equal to 5% was assumed. To verify the hypothesis that the models are statistically equal to the experimental values, it was necessary to check the normal distribution hypothesis for the dynamic models and experimental results. Because these p-values are lower than α, we can reject the hypothesis of normality in the samples. Therefore, to test the hypothesis that the samples were from the same population, the Mann–Whitney U test was performed. The p-values are listed in Table 17.

Table 17. Normality and median p-value results.

	Normality test	Mann–Whitney test
Experimental	0.01%	—
F3D	0.02%	8.86%
F4D	0.01%	6.87%
Bio	0.01%	19.76%
FSV	0.01%	10.80%
PB	0.02%	5.79%
SFF	0.04%	3.50%
HI1.12	0.02%	1.03%

For the single foot force model [39] and the Heel Impact model [6] with f_{mi} = 1.12, the p-values are lower than α. Therefore, the hypothesis that these models statistically equal the experimental values can be rejected. The p-values of the other dynamic models do not allow rejection of this hypothesis. Therefore, there is a higher certainty that the biodynamic model [46] is more similar to the reference values, followed by the model proposed by Varela et al. [40].

4 FINAL REMARKS AND CONCLUSIONS

This study presents an extensive dynamic analysis of composite steel and concrete floors subjected to human walking activities, and aims to define a dynamic model that is more similar to the experimental values in terms of acceleration results for different floor conditions.

Based on the simulated composite steel and concrete floors, it was observed that the application of the Fourier series with only one point load in the center of the walking path is not adequate to represent walking activities, and leads to high error values, such as an RMSE parameter of 159.29% for peak acceleration. In general, the Fourier series considering temporal and spatial variations presented acceleration results that were higher than the reference results. In particular, for step frequencies near 2.0 Hz, the numerical model yielded results that are close to the experimental results. The use of four harmonics had a relatively insignificant influence on the acceleration response, which may be explained by the harmonic analysis, but requires a higher computational cost.

The biodynamic model [46] provided the best peak acceleration analysis results for points in the walking path among all the simulations performed. The results were corroborated based on the PBIAS and Mann–Whitney tests, which presented the best values in these analyses and the second-best value for the RMSE parameter. The model proposed by Varela et al. [40] was the second-best model, with the lowest value for the RMSE parameter, and the second-best model in the PBIAS and Mann–Whitney U analyses. Therefore, for peak acceleration analysis at points along the walking path, these dynamic models are recommended.

However, for the investigated floors, when analyzing points outside the walking path, all dynamic models presented results below the experimental ones, and their use is not recommended for analyzing vibrations in adjacent bays. This may be explained by the hypothesis used during model calibration, which considered the results of the walking path.

For the RMS acceleration analysis of the investigated floors, only the single foot force model [39] led to adequate results, which were corroborated by the PBIAS and RMSE parameters. The other models achieved RMS acceleration results that were below the reference values.

ACKNOWLEDGMENTS

The authors acknowledge the PROEF and PDPG grant provided to the Post-Graduation Program in Civil Engineering (PROEC/UFS) by the Fundação de Apoio à Pesquisa e a Inovação Tecnológica do Estado de Sergipe/Coordenação de Aperfeiçoamento de Pessoal de Nível Superior (FAPITEC/CAPES), the Laboratory of Mathematical Modelling in Civil Engineering (LAMEC) of the Disaster Research Institute (IPD/UFS) for physical support during the development of this study, and CAPES for financial support for the M.Sc. studies.

REFERENCES

[1] W. G. Machado, A. R. Silva, and F. A. Neves, " Dynamic analysis of composite beam and floors with deformable connection using plate, bar and interface elements," *Eng. Struct.*, vol. 184, pp. 247–256, 2019, http://doi.org/10.1016/j.engstruct.2019.01.070.

[2] M. S. Gonçalves, A. Pavic, and R. L. Pimentel, "Vibration serviceability assessment of office floors for realistic walking and floor layout scenarios: literature review," *Adv. Struct. Eng.*, vol. 23, no. 6, pp. 1238–1255, 2020, http://doi.org/10.1177/1369433219888753.

[3] Z. Muhammad, P. Reynolds, O. Avci, and M. Hussein, "Review of pedestrian load models for vibration serviceability assessment of floor structures," *Vibration*, vol. 2, no. 1, pp. 1–24, 2018, http://doi.org/10.3390/vibration2010001.

[4] H. Bachmann and W. Ammann, *Vibrations in Structures Induced by Man and Machines*, 3rd ed. Zürich: Int. Assoc. Bridge Struct. Eng., 1987.

[5] J. S. Knudsen, N. Grathwol, and S. O. Hansen, "Vibrational response of structures exposed to human-induced loads," *Dyn. Civ. Struct*, vol. 2, pp. 151–158, 2019, http://doi.org/10.1007/978-3-319-74421-6_20.

[6] W. D. Varela and R. C. Battista, "Um modelo para estimativa realista das vibrações em estruturas induzidas por pessoas caminhando," *Rev Sul Am Eng Estrutural*, vol. 6, pp. 91–123, 2009, http://dx.doi.org/10.5335/rsee.v6i1.1509.

[7] T. M. Murray, D. E. Allen, E. E. Ungar, and D. B. Davis, *Vibrations of Steel-Framed Structural Systems Due to Human Activity*, 2nd ed. Chicago: Am. Inst. Steel Constr., 2016.

[8] W. D. Varela and R. C. Battista, "Control of vibrations induced by people walking on large span composite floor decks," *Eng. Struct.*, vol. 33, no. 9, pp. 2485–2494, 2011, http://doi.org/10.1016/j.engstruct.2011.04.021.

[9] L. Wang, S. Nagarajaiah, Y. Zhou, and W. Shi, "Experimental study on adaptive-passive tuned mass damper with variable stiffness for vertical human-induced vibration control," *Eng. Struct.*, vol. 280, pp. 115714, 2023, http://doi.org/10.1016/j.engstruct.2023.115714.

[10] L. M. Hanagan and M. C. Chattoraj, “A whole building cost perspective to floor vibration serviceability,” in *Proc. Build. Integr. Solutions*, Omaha, 2006. http://doi.org/10.1061/40798(190)37.

[11] D. E. Allen, J. H. Rainer, and G. Pernica, "Vibration criteria for assembly occupancies," *Can. J. Civ. Eng.*, vol. 12, no. 3, pp. 617–623, 1985, http://doi.org/10.1139/l85-069.

[12] S. E. Mouring and B. R. Ellingwood, "Guidelines to minimize floor vibrations from building occupants," *J. Struct. Eng.*, vol. 120, no. 2, pp. 507–526, 1994, http://doi.org/10.1061/(ASCE)0733-9445(1994)120:2(507).

[13] T. A. Wyatt, *Design Guide on the Vibration of Floors*. London: Steel Constr. Inst., 1989.

[14] A. L. Smith, S. J. Hicks, and P. J. Devine, *Design of Floors for Vibration: a New Approach*. London: Steel Constr. Inst., 2009.

[15] International Organization for Standardization, *Evaluation of Human Exposure to Whole-Body Vibration – Part 2: Human Exposure to Continuous and Shock-Induced Vibrations in Buildings (1 to 80 Hz)*, ISO 2631-2, 1989.

[16] J. H. Rainer, G. Pernica, and D. E. Allen, "Dynamic loading and response of footbridges," *Can. J. Civ. Eng.*, vol. 15, no. 1, pp. 66–71, 1988, http://doi.org/10.1139/l88-007.

[17] W. E. Saul and C. Y. Tuan, "Review of live loads due to human movements," *J. Struct. Eng.*, vol. 112, no. 5, pp. 995–1004, 1986, http://doi.org/10.1061/(ASCE)0733-9445(1986)112:5(995).

[18] S. V. Ohlsson, “Floor vibrations and human discomfort,” M.S. thesis, Chalmers Univ. Technol., Gothenburg, 1982.

[19] J. M. Brownjohn, A. Pavic, and P. Omenzetter, "A spectral density approach for modelling continuous vertical forces on pedestrian structures due to walking," *Can. J. Civ. Eng.*, vol. 31, no. 1, pp. 65–77, 2004, http://doi.org/10.1139/l03-072.

[20] A. Ebrahimpour, A. Hamam, R. L. Sack, and W. N. Patten, "Measuring and modeling dynamic loads imposed by moving crowds," *J. Struct. Eng.*, vol. 122, no. 12, pp. 1468–1474, 1996, http://doi.org/10.1061/(ASCE)0733-9445(1996)122:12(1468).

[21] F. T. Silva, H. M. B. F. Brito, and R. L. Pimentel, "Modeling of crowd load in vertical direction using biodynamic model for pedestrians crossing footbridges," *Can. J. Civ. Eng.*, vol. 40, no. 12, pp. 1196–1204, 2013, http://doi.org/10.1139/cjce-2011-0587.

[22] M. S. Pfeil, W. D. Varela, and N. D. P. A. Costa, "Experimental calibration of a one degree of freedom biodynamic model to simulate human walking-structure interaction," *Eng. Struct.*, vol. 262, pp. 114330, 2022, http://doi.org/10.1016/j.engstruct.2022.114330.

[23] L. Cao, J. Li, Y. F. Chen, and S. Huang, "Measurement and application of walking models for evaluating floor vibration," *Structures*, vol. 50, pp. 561–575, 2023, http://doi.org/10.1016/j.istruc.2023.02.073.

[24] K. van Nimmen, G. Lombaert, I. Jonkers, G. De Roeck, and P. van den Broeck, "Characterisation of walking loads by 3D inertial motion tracking," *J. Sound Vibrat.*, vol. 333, no. 20, pp. 5212–5226, 2014, http://doi.org/10.1016/j.jsv.2014.05.022.

[25] K. van Nimmen, P. Verbeke, G. Lombaert, G. De Roeck, and P. van den Broeck, "Numerical and experimental evaluation of the dynamic performance of a footbridge with tuned mass dampers," *J. Bridge Eng.*, vol. 21, no. 8, pp. C4016001, 2016, http://doi.org/10.1061/(ASCE)BE.1943-5592.0000815.

[26] M. Kasperski, "Realistic simulation of a random pedestrian flow," *Procedia Eng.*, vol. 199, pp. 2814–2819, 2017, http://doi.org/10.1016/j.proeng.2017.09.341.

[27] P. Wang and J. Chen, "Floor modal mass identification using human-induced dynamic excitation," *Measurement*, vol. 217, pp. 113038, 2023, http://doi.org/10.1016/j.measurement.2023.113038.

[28] Y. G. M. Fahmy and A. N. M. Sidky, "An experimental investigation of composite floor vibration due to human activities: a case study," *HBRC J.*, vol. 8, no. 3, pp. 228–238, 2012, http://doi.org/10.1016/j.hbrcj.2012.12.001.

[29] A. R. Barrett, “Dynamic testing of in-situ composite floors and evaluation of vibration using the finite element method,” Ph.D. dissertation, Fac. Virginia Polytech. Inst. State Univ., Virginia, 2006.

[30] D. B. Davis, “Finite element modeling for prediction of low frequency floor vibrations due to walking,” Ph.D. dissertation,” Fac. Virginia Polytech. Inst. State Univ., Virginia, 2008.

[31] D. Liu and D. B. Davis, "Walking vibration response of high-frequency floors supporting sensitive equipment," *J. Struct. Eng.*, vol. 141, no. 8, pp. 04014199, 2015, http://doi.org/10.1061/(ASCE)ST.1943-541X.0001175.

[32] B. E. Ferreira, H. Carvalho, J. G. S. D. Silva, R. B. Caldas, and J. V. Aguiar, "Experimental evaluation of induced human walking vibrations on steel-concrete composite floors," *Rev. IBRACON Estrut. Mater.*, vol. 14, no. 4, e14406, 2021, http://doi.org/10.1590/s1983-41952021000400006.

[33] L. A. D. Silva Jr. and J. F. A. Pinto, "Experimental analysis of walking induced vibrations in composite floor and performance evaluation considering human comfort," *Ambient. Constr.*, vol. 23, no. 1, pp. 131–144, 2022, http://doi.org/10.1590/s1678-86212023000100653.

[34] J. Aguiar, B. Ferreira, H. Carvalho, and J. G. S. Silva, "Assessment of steel-concrete composite floors dynamic response when subjected to people walking," *Ce Pap.*, vol. 6, no. 3–4, pp. 2388–2393, 2023, http://doi.org/10.1002/cepa.2713.

[35] A. V. A. Mello, J. G. S. Silva, P. C. G. S. Vellasco, S. A. L. Andrade, and L. R. O. Lima, "Dynamic analysis of composite systems made of concrete slabs and steel beams," *J. Construct. Steel Res.*, vol. 64, no. 10, pp. 1142–1151, 2008, http://doi.org/10.1016/j.jcsr.2007.09.011.

[36] F. P. Figueiredo, J. G. S. Silva, L. R. O. Lima, P. C. G. S. Vellasco, and S. A. L. Andrade, "A parametric study of composite footbridges under pedestrian walking loads," *Eng. Struct.*, vol. 30, no. 3, pp. 605–615, 2008, http://doi.org/10.1016/j.engstruct.2007.04.021.

[37] F. F. Campista and J. G. S. Silva, "Vibration analysis of steel concrete composite floors when subjected to rhythmic human activities," *J Civ Struct Heal Monit*, vol. 8, no. 5, pp. 737–754, 2018, http://doi.org/10.1007/s13349-018-0303-6.

[38] S. C. Kerr, “Human induced loading on staircases,” Ph.D. dissertation,” Univ. Coll. London, London, 1998.

[39] Q. Li, J. Fan, J. Nie, Q. Li, and Y. Chen, "Crowd-induced random vibration of footbridge and vibration control using multiple tuned mass dampers," *J. Sound Vibrat.*, vol. 329, no. 19, pp. 4068–4092, 2010, http://doi.org/10.1016/j.jsv.2010.04.013.

[40] W. D. Varela, M. S. Pfeil, and N. P. A. Costa, "Experimental investigation on human walking loading parameters and biodynamic model," *J Vib Eng Technol*, vol. 8, no. 6, pp. 883–892, 2020, http://doi.org/10.1007/s42417-020-00197-3.

[41] R. Sachse, A. Pavic, and P. Reynolds, “The influence of a group of human occupants on modal properties of a prototype assembly structure,” in *Proc. 5th Eur. Conf. Dyn. EURODYN*, Munich, Germany, 2002.

[42] E. Shahabpoor, A. Pavic, and V. Racic, "Identification of mass-spring-damper model of walking humans," *Structures*, vol. 5, pp. 233–246, 2016, http://doi.org/10.1016/j.istruc.2015.12.001.

[43] C. Bedon, "Single body sensor for calibration of spring-mass-damper parameters in biodynamic pedestrian modelling," *Measurement*, vol. 218, pp. 113258, 2023, http://doi.org/10.1016/j.measurement.2023.113258.

[44] E. Shahabpoor and A. Pavic, "Human-structure dynamic interactions: identification of two-degrees-of-freedom walking human model," *J. Sound Vibrat.*, vol. 569, pp. 117974, 2024, http://doi.org/10.1016/j.jsv.2023.117974.

[45] I. Roupa, M. R. Silva, F. Marques, S. B. Gonçalves, P. Flores, and M. T. Silva, "On the modeling of biomechanical systems for human movement analysis: a narrative review," *Arch. Comput. Methods Eng.*, vol. 29, no. 7, pp. 4915–4958, 2022, http://doi.org/10.1007/s11831-022-09757-0.

[46] M. A. Toso, H. M. Gomes, F. T. Silva, and R. L. Pimentel, "Experimentally fitted biodynamic models for pedestrian-structure interaction in walking situations," *Mech. Syst. Signal Process.*, vol. 72–73, pp. 590–606, 2016, http://doi.org/10.1016/j.ymssp.2015.10.029.

[47] S. Živanović, A. Pavić, and P. Reynolds, "Probability-based prediction of multi-mode vibration response to walking excitation," *Eng. Struct.*, vol. 29, no. 6, pp. 942–954, 2007, http://doi.org/10.1016/j.engstruct.2006.07.004.

[48] ANSYS, *Fluent User's Guide*. Canonsburg, 2013.

[49] R. W. Clough and J. Penzien, *Dynamics of Structures*, 3rd ed. Berkeley: Computers & Structures, Inc., 2003.

Author contributions: R.N. Cunha: conceptualization, formal analysis, methodology, writing; H.S.D. Argôlo: conceptualization, formal analysis, methodology, writing, supervision.

Editors: Sergio Hampshire C. Santos, Daniel Carlos Taissum Cardoso.